

Suitability of a thermoelectric power generator for implantable medical electronic devices

Yang Yang¹, Xiao-Juan Wei¹ and Jing Liu^{1,2,3}

¹ Technical Institute of Physics and Chemistry, Chinese Academy of Sciences, Beijing 100080, People's Republic of China

² School of Medicine, Biomedical Engineering Department, Tsinghua University, Beijing 100084, People's Republic of China

E-mail: jliu@cl.cryo.ac.cn

Received 18 April 2007, in final form 26 July 2007

Published 30 August 2007

Online at stacks.iop.org/JPhysD/40/5790

Abstract

Embedding a thermoelectric generator (TEG) in a biological body is a promising way to supply electronic power in the long term for an implantable medical device (IMD). The unique merit of this method lies in its direct utilization of the temperature difference intrinsically existing throughout the whole biological body. However, little is known about the practicability of such a power generation strategy up to now. This paper attempts to evaluate the energy generation capacity of an implanted TEG subject to various physiological or environmental thermal conditions. Through theoretical analysis, it was found that the highest temperature gradient occurs near the skin surface of the human body, which suggested a candidate site for implanting and positioning the TEG. In addition, numerical simulations were performed on three-dimensional bioheat transfer problems in human bodies embedded with TEGs at different implantation depths and configurations. To further enhance energy generation of an implanted TEG, several external technical approaches by intentionally cooling or heating the skin surface were proposed and evaluated. Conceptual experiments either *in vitro* or *in vivo* were implemented to preliminarily test the theoretical predictions. Given the fact that an IMD generally require very little working energy, the TEG could serve well as a potential long-term energy supplier for such medical practices.

(Some figures in this article are in colour only in the electronic version)

1. Introduction

Implantable medical devices (IMDs) have had a long history of outstanding success in clinical practice. They are extremely important today as a part of modern advanced medical technologies. Enhancing or replacing certain functions of a specific tissue or organ in the human body is their distinct clinical role. In fact, such devices have already been beneficial not only to the patient but also to healthy people who wish to adopt them to expand their biological limits in the near future. Some IMDs are already very familiar to us, such as cardiac

pacemakers, cardiac defibrillators, cochlear implants and so on [1, 2].

Among the many factors affecting the performance of an IMD, energy supply is always a major concern. There is often a mismatch between the patient's lifetime and the service life of an IMD. This issue is caused mainly by the batteries since other parts seldom have a problem of abrasion. In the 1980s, over 95% of IMDs were powered by lithium batteries whose service life had originally been rated as 10 years [3]. Unfortunately, it turned out later that many patients every year had to undergo surgery to check on the performance of the IMD or replace it with new one. Therefore, extending the

³ Author to whom any correspondence should be addressed.

service life of batteries in implanted devices has become a rather important issue. Many efforts have been intensely made towards this goal but the situation remains largely unchanged. For instance, attention has always been paid to bio-fuel cells, on the assumption that one can use glucose as fuel in the body for an IMD [4]. At the same time, nuclear cells for pacemakers also attract much attention owing to their safety and reliability in supplying power [5]. Nevertheless, these methods have certain inherent drawbacks such as potential contamination, high cost or just insufficient performance etc. Therefore, finding an alternative long-term source of electricity supply will partially address the urgent need in this area. Among the various renewable power sources, the thermoelectric micro-generator is a promising candidate because of its excellent features in terms of reliable performance, long duration and the possibility of getting energy directly from the body heat [6].

The basic thermoelectric phenomena, such as the Peltier effect, and their macroscopic thermodynamic behaviours were first investigated between the 1820s and the 1850s. However, the corresponding technology was not fully used for a rather long time. Until the 1950s, the advent of doped semiconductor materials with small band gap, which were found to have much greater thermoelectric performances than the pure metals, revived the interest in this field. Recently, driven by the need to find a green and low cost method of energy generation, exploitation of the thermoelectric generator (TEG) has become a pretty hot topic throughout the world [7, 8]. During the past four decades, TEGs have been used practically in a wide variety of fields [8]. In such devices, when a temperature difference is established between its hot and cold junctions, a Seebeck voltage directly proportional to this temperature difference is generated [7]. This consists of one of the most commonly encountered situations for application. For medical purposes, using a person's body heat to power a TEG and then to drive a wristwatch using a person's body heat has been demonstrated as a first commercial sample and several approaches to building high performance TEGs via micromachining techniques are now available [6, 9, 10].

This paper is dedicated to investigating the energy generation behaviour of an implanted TEG which employs the undeniable temperature differences between the body core and the skin surface. Parametric simulations and a series of experiments were performed on some typical cases with varied transplanted depths and configurations of a TEG to evaluate its suitability for power generation. To the best of the authors' knowledge, such efforts have not been undertaken before.

2. Theoretical analysis and numerical simulation

2.1. Maximum temperature gradient across human body

A typical implanting pattern for the TEG can be illustrated by figure 1(a), which is similar to an IMD. The TEG was embedded into the human body to directly utilize the heat there, i.e. the temperature difference between the body core and the skin surface. For the sake of convenience in calculation, the human body is simplified as a three-layer model consisting of muscle, fat and skin layer, respectively. The blue block structure embedded in the muscle tissue denotes the TEG.

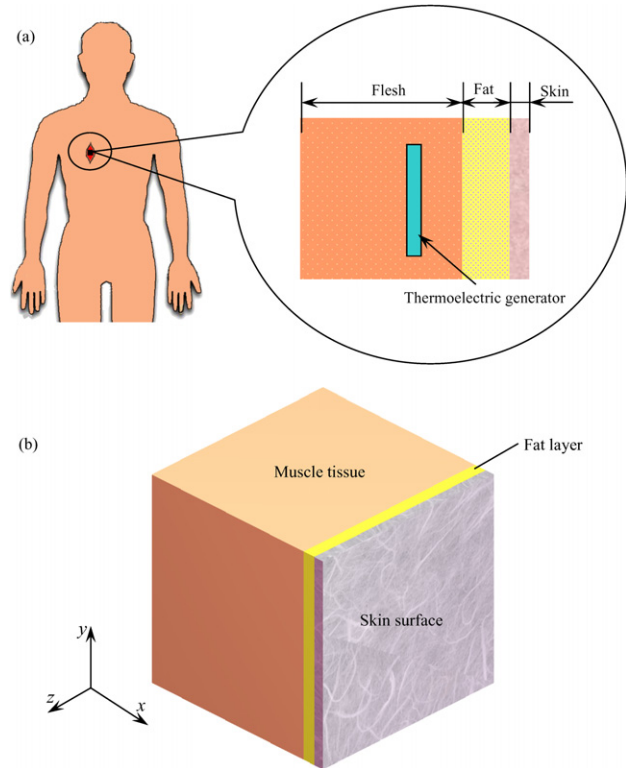


Figure 1. (a) Simplified three-layer human body tissues with an embedded TEG and (b) sketch of the 3D cubic calculation domain of size $0.08 \text{ m} \times 0.08 \text{ m} \times 0.08 \text{ m}$.

The electrical voltage gained between the two junctions of the TEG could be generally characterized by the following equation [11],

$$V_{\text{output}} = n\Delta T(\alpha_1 - \alpha_2), \quad (1)$$

where V_{output} is output voltage from the TEG, ΔT is temperature difference across the two junctions of the TEG, n is the number of thermocouples that are electrically connected in series and α_1 , α_2 are the Seebeck coefficients of TEG thermoelements, respectively.

Equation (1) presents the basic equation for correlating the output voltage from a TEG (without load) and the temperature difference across it. Clearly, the voltage depends on both n , α_1 , α_2 and ΔT . n , α_1 and α_2 are the intrinsic properties of a TEG device. Therefore, evaluating the magnitude of ΔT will provide important information on the electrical energy generation capability. This will be done by a group of different bioheat transfer analyses on the biological body either with or without a TEG embedded.

Considering a generalized one-dimensional (1D) heat transfer case in steady state, the temperature difference across the two junctions of a TEG can be approximately described by

$$\Delta T = \frac{q\delta}{k_t}, \quad (2)$$

where q is the heat flux arriving at the hot junction from the interior tissue side, and δ , k_t denote the thickness and thermal conductivity of the TEG, respectively. It is obvious that the temperature difference ΔT which determines the output

voltage depends only on the heat flux from the tissue since δ and k_t are the own properties of a TEG.

In the following, a 1D bioheat transfer model without a TEG embedded will first be adopted for simplicity to evaluate which part of the tissues would have the maximum temperature gradient. To characterize heat transfer in the living tissues, the well-known Pennes bioheat equation [12] was used, which describes the influence of blood flow on the temperature distribution in the tissue in terms of volumetrically distributed heat sinks or sources, i.e.

$$\rho c \frac{\partial T(x, t)}{\partial t} = k \frac{\partial^2 T(x, t)}{\partial x^2} + Q_b + Q_m, \quad (3)$$

where $Q_b = \rho_b c_b \omega_b (T_a - T(x, t))$; ρ , c are, respectively, the density and specific heat of tissue; ρ_b , c_b and ω_b denote the density, specific heat and perfusion rate of blood; k is the thermal conductivity of tissue; T_a is the arterial temperature, which is often treated as a constant, T is the tissue temperature and Q_m is the metabolic heat generation rate.

The steady-state temperature field for the basal state of biological bodies can then be obtained by solving the following equations:

$$\begin{cases} k \frac{d^2 T_0(x)}{dx^2} + \omega_b \rho_b c_b [T_a - T_0(x)] + Q_m = 0, \\ T_0(x) = T_c, & x = 0, \\ -k \frac{dT_0(x)}{dx} = h_0 [T_f - T_0(x)], & x = L, \end{cases} \quad (4)$$

where $T(x, 0) = T_0(x)$ is the steady-state temperature fields, T_c is the body core temperature and often regarded as a constant, h_0 is the apparent heat convection coefficient between the skin surface and the surrounding air under the physiologically basal state and is overall a contribution from natural convection and radiation and T_f is the surrounding air temperature. Here, the skin surface is defined at $x = L$ and the body core at $x = 0$.

The analytical solution to equation (4) has been obtained in [13] from which the heat flux at any tissue position x could be written as

$$\begin{aligned} q(x) = -k \frac{dT(x)}{dx} = -k \left\{ \left[A \left(T_c - T_a - \frac{Q_m}{\omega_b \rho_b c_b} \right) \text{sh}(\sqrt{A}x) \right. \right. \\ \left. \left. + \left[\frac{h_0 \sqrt{A}}{k} (T_f - T_c) \right] \text{ch}(\sqrt{A}x) \right] \right. \\ \left. \times \left[\sqrt{A} \text{ch}(\sqrt{A}L) + \frac{h_0}{k} \text{sh}(\sqrt{A}L) \right]^{-1} \right\}, \quad (5) \end{aligned}$$

where $A = \omega_b \rho_b c_b / k$.

The derivative of the heat flux can then be expressed as

$$\begin{aligned} q'(x) = \frac{dq(x)}{dx} = -k \left\{ \left[A \sqrt{A} \left(T_c - T_a - \frac{Q_m}{\omega_b \rho_b c_b} \right) \text{ch}(\sqrt{A}x) \right. \right. \\ \left. \left. + \left[\frac{h_0 A}{k} (T_f - T_c) \right] \text{sh}(\sqrt{A}x) \right] \right. \\ \left. \times \left[\sqrt{A} \text{ch}(\sqrt{A}L) + \frac{h_0}{k} \text{sh}(\sqrt{A}L) \right]^{-1} \right\}. \quad (6) \end{aligned}$$

In equation (6), T_c and T_a are often treated as equal to 310 K, and T_f is generally less than T_c . It can thus be easily found that

$q'(x)$ is permanently larger than zero. In other words, the heat flux $q(x)$ is always a monotonic increasing quantity with the dimension x , which means the heat flux $q(x)$ would reach its maximum value at the position farthest from the body core.

Based on the above theoretical prediction, a conclusion can be drawn as follows. When implanting a TEG, the best place should be as close as possible to the superficial skin, where a maximum temperature difference between the two junctions of the TEG could be established. This would guarantee a good output of the TEG.

2.2. Numerical simulation

2.2.1. Theoretical model. Although a brief evaluation of the heat transfer in the human body has already been given as above, it represents overall only a highly simplified 1D case. A better understanding of the actual conditions requires a three-dimensional (3D) numerical simulation on the heat transfer problems of the human body embedded either with or without a TEG. For this purpose, a rectangular geometry is selected for the analysis. The calculation domain is prescribed in a $0.08 \text{ m} \times 0.08 \text{ m} \times 0.08 \text{ m}$ cube, where x denotes the tissue depth from the body core while y and z are coordinates along the surface (figure 1(b)).

The heat transfer in a TEG can be described by a thermal diffusion equation:

$$\rho_t c_t \frac{\partial T_t(X, t)}{\partial t} = \nabla k_t \nabla [T_t(X, t)], \quad (7)$$

where ρ_t , c_t , k_t are, respectively, the density, specific heat and thermal conductivity of the material of the TEG; X contains the Cartesian coordinates x , y and z ; $T_t(X, t)$ is the device temperature. Here, the self Joule heating of the TEG and heat transfer by the Peltier effect during working were not specifically considered for simplicity.

The 3D Pennes equation for characterizing bioheat transfer of the surrounding tissues reads as

$$\rho c \frac{\partial T(X, t)}{\partial t} = \nabla k(X) \nabla [T(X, t)] + Q_b + Q_m, \quad (8)$$

where $T(X, t)$ is the tissue temperature distribution and $k(X)$ the space-dependent thermal conductivity of the tissue. $Q_b = \rho_b c_b \omega_b(X) (T_a - T(X, t))$, and $\omega_b(X)$ is the space-dependent blood perfusion. In the present model, blood perfusion and metabolic heat generation exist only in the muscle tissue.

The boundary conditions for a practical TEG implantation pattern as shown in figure 1(b) are prescribed as follows:

$$-k \frac{\partial T}{\partial y} = 0 \quad \text{at } y = 0, \quad -k \frac{\partial T}{\partial y} = 0 \quad \text{at } y = L, \quad (9)$$

$$-k \frac{\partial T}{\partial z} = 0 \quad \text{at } z = 0, \quad -k \frac{\partial T}{\partial z} = 0 \quad \text{at } z = L, \quad (10)$$

$$T = T_c \quad \text{at } x = 0, \quad -k \frac{\partial T}{\partial x} = h_0 (T_f - T) \quad \text{at } x = L, \quad (11)$$

where L is the length of the calculation domain.

The reason for adopting the adiabatic conditions on the boundaries along the y and z directions is based on the consideration that at the positions far from the centre of

the domain, the temperature field is almost unaffected by the central domain or external heating/cooling.

At the six interfaces between biological tissues and the rectangular TEG, a continuum equation for both temperature and heat flux is adopted, i.e.

$$T = T_t, \quad k \frac{\partial T}{\partial n} = k_t \frac{\partial T_t}{\partial n}, \quad (12)$$

where T_t and k_t are, respectively, temperature and thermal conductivity of the TEG, n is the normal direction of the tissue–TEG interface.

In the numerical calculations, the typical parameters for the tissues are set as follows [14]: $\rho = \rho_b = 1000 \text{ kg m}^{-3}$, $c = c_b = 4200 \text{ J kg}^{-1} \text{ K}^{-1}$. The muscle tissue is regarded to have a thickness of 71 mm with thermal parameters as $k = 0.5 \text{ W m}^{-1} \text{ K}^{-1}$, $Q_m = 420 \text{ W m}^{-3}$, $\omega_b = 0.0005 \text{ ml s}^{-1} \text{ ml}^{-1}$. The thickness of the skin is generally within the range 0.5–4 mm and treated here as 4 mm. Its thermal conductivity is $0.3 \text{ W m}^{-1} \text{ K}^{-1}$. The thickness of the fat layer is taken as 5 mm, and its thermal conductivity is $0.2 \text{ W m}^{-1} \text{ K}^{-1}$. Both Q_m and ω_b in these two layers are zero. The body core temperature is set as $T_c = 310 \text{ K}$.

For the TEG part, the bismuth telluride has been selected as the material whose typical parameters are set as $\rho_t = 7700 \text{ kg m}^{-3}$, $c_t = 500 \text{ J kg}^{-1} \text{ K}^{-1}$, $k_t = 1.35 \text{ W m}^{-1} \text{ K}^{-1}$, respectively [11, 15]. Although various materials can be tested using this method, only the above material will be analysed for brevity.

2.2.2. Validation of numerical scheme. The first calculation was performed to validate the current numerical scheme. As a benchmark, the 1D Pennes analytical solution as derived above was adopted. The 3D numerical simulations coupled with the heat transfer equations in tissue and the TEG were developed from the commercially available software FLUENT in a $0.08 \text{ m} \times 0.08 \text{ m} \times 0.08 \text{ m}$ cube with the same parameters and boundary conditions given above. The heat transfer coefficient is set as $20 \text{ W m}^{-2} \text{ K}^{-1}$ and the environmental temperature is 288 K. Presented in figure 2(a) is a comparison for 1D steady-state temperature distribution along the x direction between the analytical solution and the numerical simulation for the case without embedding a TEG in the tissue. Figure 2(b) is for the derivative of figure 2(a) which illuminates the existence of a temperature difference from the body core to the skin surface. Clearly, the two kinds of solutions agree with each other very well. Besides, the heat flux increases with the distance from the body core, which has also been revealed by the previous theoretical analysis. This guarantees that the 3D simulation as given below will be approximately true.

2.2.3. Typical temperature distribution in 3D tissues. The first calculation was made in the cubic domain $0.08 \text{ m} \times 0.08 \text{ m} \times 0.08 \text{ m}$ including the three-layer as depicted in figure 3(a), which however has not been implanted with a TEG. The skin surface was described as a convective boundary condition with a heat transfer coefficient of $20 \text{ W m}^{-2} \text{ K}^{-1}$ and an environmental temperature of 288 K. The steady-state temperature distribution on the middle Z-cross section is shown in figure 4(a).

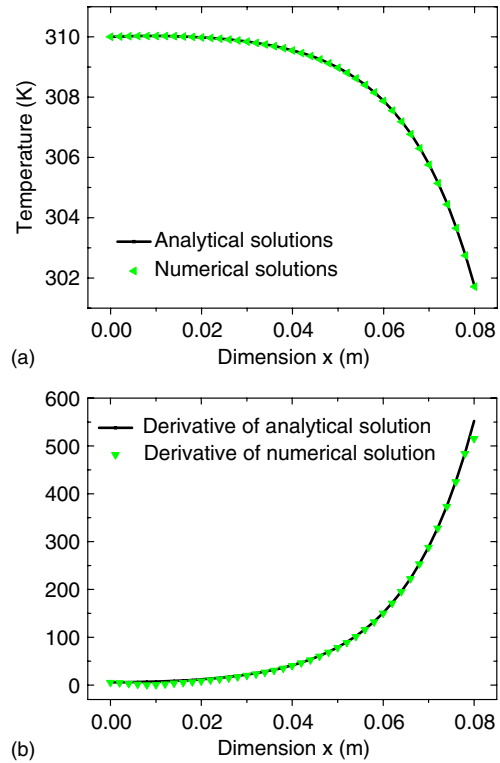


Figure 2. (a) Steady-state temperature distribution along the dimension x in muscle tissue ($h_f = 20 \text{ W m}^{-2} \text{ K}^{-1}$, $T_c = 288 \text{ K}$) and (b) derivative of (a).

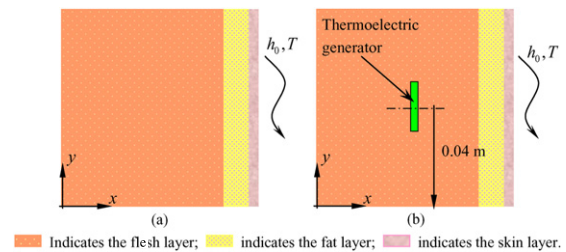


Figure 3. Sketch of the calculation domain for the cases without (a) or with (b) TEG.

For the implanting case, the size of the TEG was set as a $20 \text{ mm} \times 20 \text{ mm} \times 3 \text{ mm}$ thin cube as shown in figure 3(b) and the skin surface was also subjected to the same convective boundary condition. In order to test the temperature difference formed across the TEG with different implantation positions, several distances between the hot junction of the TEG and the body core along dimension x are, respectively, prescribed as 0.02 m, 0.04 m, 0.05 m, 0.06 m and 0.071 m. The results in figure 4(b) indicate that no matter where the implanted TEG is located, there always exists a temperature difference between its two junctions. The largest temperature difference is 0.482 K, which occurs at the point farthest from the body core. Coincidentally, figure 4(c) depicts the steady-state temperature distribution on the middle Z-cross section with TEG embedded, which is obviously different from figure 4(a). Due to embedding of the TEG and its different thermal properties from the surrounding tissues, the isotherm in figure 4(c) appears somewhat different from that in figure 4(a). It tends to bend across the TEG.

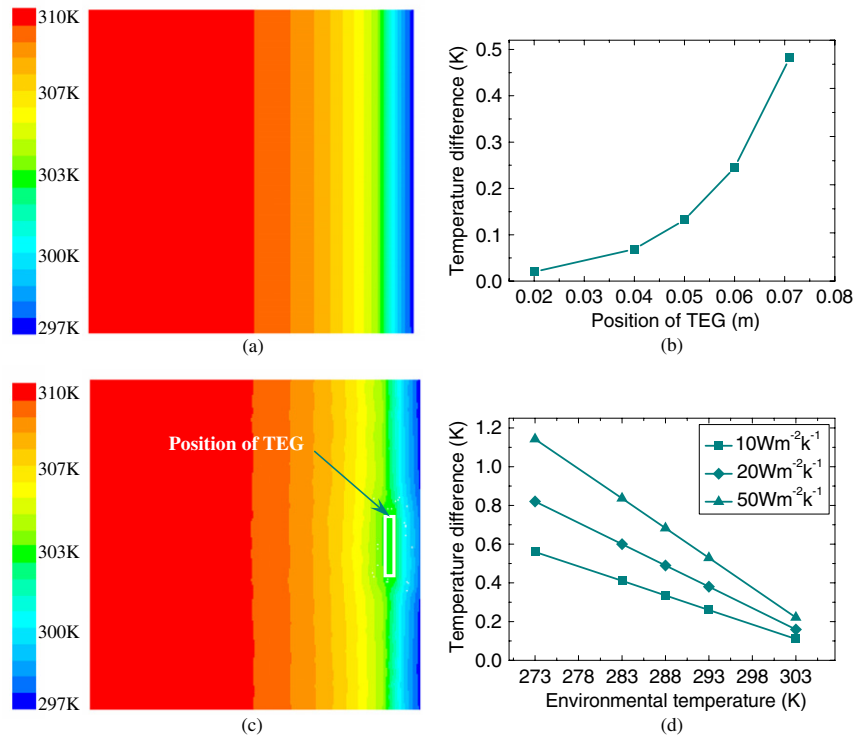


Figure 4. Temperature differences across the two junctions of TEG. (a) Steady-state temperature distribution on the middle Z-cross section without embedding TEG; (b) $h_0 = 20 \text{ W m}^{-2} \text{ K}^{-1}$, $T_f = 288 \text{ K}$; position: $x = 0.02 \text{ m}$, 0.04 m , 0.05 m , 0.06 m , 0.071 m , respectively, with TEG; (c) steady-state temperature distribution on the middle Z-cross section with TEG at position: $x = 0.071 \text{ m}$ and (d) position: $x = 0.071 \text{ m}$; $h_0 = 10, 20, 50 \text{ W m}^{-2} \text{ K}^{-1}$; $T_f = 273 \text{ K}$, 283 K , 288 K , 293 K , 298 K and 303 K , respectively.

To test the effects of various environmental conditions, more simulations were also made by setting the heat transfer coefficient as $10 \text{ W m}^{-2} \text{ K}^{-1}$, $20 \text{ W m}^{-2} \text{ K}^{-1}$, $50 \text{ W m}^{-2} \text{ K}^{-1}$ and treating the environmental temperature as 273 K , 283 K , 288 K , 293 K and 303 K , respectively. The calculated results are presented in figure 4(d). Clearly, for the same heat transfer coefficient, the largest temperature difference occurred in the case with the lowest environmental temperature 273 K . Under the same temperature, the largest temperature difference appears in the case with the highest heat transfer coefficient of $50 \text{ W m}^{-2} \text{ K}^{-1}$. Overall, the maximum temperature difference between the two junctions has been found as 1.142 K with $50 \text{ W m}^{-2} \text{ K}^{-1}$ heat transfer coefficients in a 273 K environment, which is already strong enough to guarantee power generation by a TEG. In fact, such situations can be still better if more powerful heat transfer enhancement strategies can be introduced in the near future.

2.2.4. Effect of physiological states on TEG electricity output. In daily life, when a person takes on various physiological states, there exists a difference between the physiological parameters. For example, the blood perfusion and metabolic heat generation, which have a significant impact on the temperature distribution in biological bodies, are widely different when a person is under different physiological activities. There exists a correlation between these two parameters [16] $W_q = \omega_b / Q_m = 1 \times 10^{-3} \text{ kg J}^{-1}$, where ω_b is the blood perfusion and Q_m the metabolic heat generation. W_q is the ratio of ω_b to Q_m . Figure 5(b) gives the temperature differences between the two junctions of a TEG by using

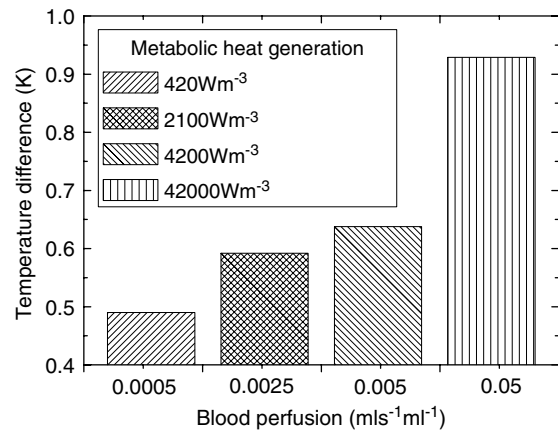


Figure 5. Temperature differences between the two junctions of TEG in different blood perfusion and metabolic heat generation rate.

different blood perfusion and metabolic heat generation rates. It suggests that the larger the blood perfusion and metabolic heat generation rate, the higher the temperature difference across the TEG that can be formed.

2.2.5. Enhancement of TEG electricity output via skin surface cooling. In order to achieve a higher temperature gradient from the body core to the skin surface, some external factors such as intentionally heating or cooling the skin surface offer valuable assistance (figure 6(a)). As the calculation shows, cooling the skin surface to 277 K can make the highest temperature difference reach 1.4 K . While heating the skin

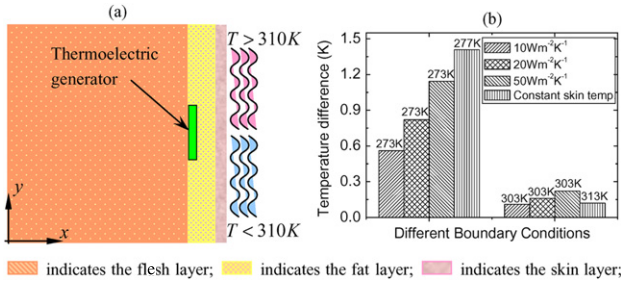


Figure 6. (a) External factors on skin surface and (b) temperature differences between the two junctions of TEG in different boundary conditions.

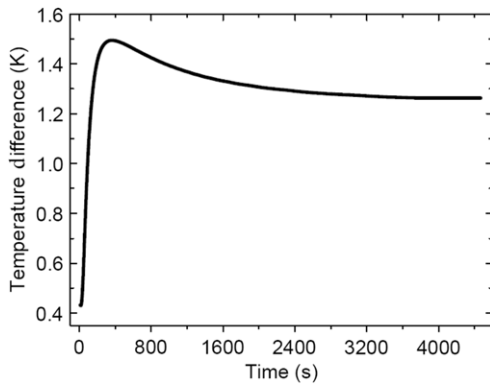


Figure 7. Transient response curve of temperature difference across TEG when cooling the skin surface.

surface to 313 K, the maximum temperature difference is only -0.119 K. Figure 6(b) is a comparison between the effects of using convective boundary and constant temperature boundary conditions at the skin surface. In the low surface temperature situation, it is obvious that the biggest temperature difference obtained by cooling the skin surface to 277 K becomes twice as large as that under the convective boundary condition with a $10 \text{ W m}^{-2} \text{ K}^{-1}$ heat transfer coefficient and a 273 K environmental temperature. Simultaneously, in the next situation, the biggest temperature difference achieved by heating the surface to 313 K is far less than the convective boundary condition with the $50 \text{ W m}^{-2} \text{ K}^{-1}$ heat transfer coefficient in a 303 K environment and even takes on an opposite temperature gradient.

Figure 7 depicts the transient response curve of the temperature difference across the TEG when cooling the skin surface. Before cooling, the tissue was regarded as being under steady state in a convective thermal environment. The heat transfer coefficient is $20 \text{ W m}^{-2} \text{ K}^{-1}$ and the environmental temperature is 288 K. When cooling the skin surface to 277 K, the temperature difference across the TEG increases rapidly and reaches its maximum value at the first 360 s. As time goes on and after establishment of the thermal equilibrium state, the temperature difference across the TEG gradually decreases and levels off. The trend is mainly attributed to the different thermal parameters between the human body and the TEG which result in the unsynchronized response to the energy transfer. Generally speaking, the response of the TEG to surface cooling is very quick and attains its charging state within 6 min.

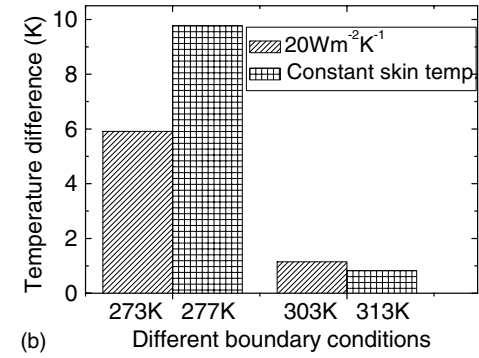
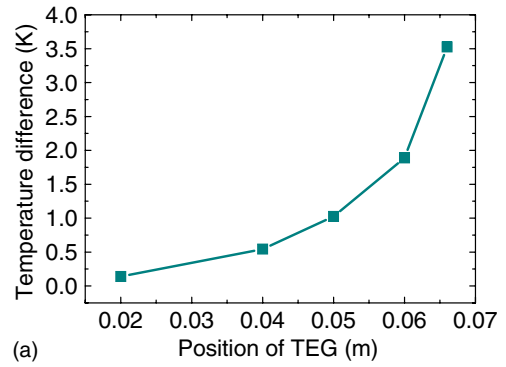


Figure 8. Temperature differences between the two junctions of TEG. (a) Using multi-stage TEG in $h_0 = 20 \text{ W m}^{-2} \text{ K}^{-1}$, $T_f = 288 \text{ K}$; position: $x = 0.02 \text{ m}$, 0.04 m , 0.05 m , 0.06 m , 0.066 m , respectively and (b) with different boundary conditions.

2.2.6. Maximizing electricity generation using multi-stage TEG. The multi-stage TEG is one kind of TEG that is made up of a group of TEGs connected in series (both electrically and spatially) with the hot junction of each TEG clinging to the cold junction of the next TEG [17] and the output is summed Seebeck voltage generated on each TEG. According to equation (2), making use of the multi-stage TEG can increase the thickness of the TEG along the direction x , which will help in realizing a much larger temperature difference. Here, a $5 \text{ mm} \times 5 \text{ mm} \times 10 \text{ mm}$ spatial domain is set as the multi-stage TEG in the calculation domain and the skin surface is also under the convective boundary condition with a heat transfer coefficient of $20 \text{ W m}^{-2} \text{ K}^{-1}$ and an environmental temperature of 288 K. The distance between the hot junction of the TEG and the body core along the x direction are prescribed, respectively, as 0.02 m, 0.04 m, 0.05 m, 0.06 m and 0.066 m. The calculations are shown in figure 8(a). The largest temperature difference is 3.5 K at the farthest position 0.066 m which is seven times larger than 0.482 K as obtained in figure 4. At the same position, when cooling the skin surface to 277 K, the highest temperature difference is 9.772 K. However, when heating the skin surface to 313 K, the highest temperature difference is only -0.852 K. Figure 8(b) displays the comparison between using convective and constant temperature boundary conditions at the skin surface. In the low surface temperature situation, when cooling the surface to 277 K, the highest temperature difference could be nearly twice as large as the result obtained with a $20 \text{ W m}^{-2} \text{ K}^{-1}$ heat transfer coefficient and a 273 K environment. Simultaneously, in the high surface temperature

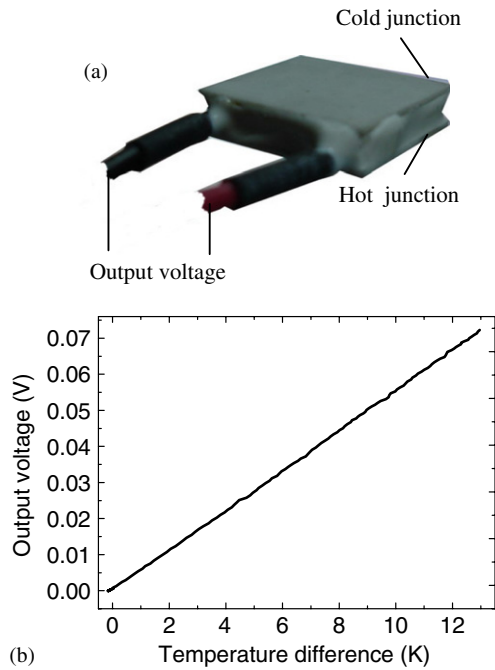


Figure 9. (a) Sketch of electricity generation experiment of a TEG and (b) relation between the temperature difference and output voltage.

situation, the highest temperature difference achieved by heating the surface to 313 K is less than the case with a $20 \text{ W m}^{-2} \text{ K}^{-1}$ heat transfer coefficient in a 303 K environment and takes on an opposite temperature gradient.

3. Experiments and results

3.1. Tests on temperature difference and energy conversion of TEG

Based on the above numerical simulation, a commercially available TEG as shown in figure 9(a) has been adopted to evaluate its real energy generation capability and then to preliminarily verify the results as predicted above. This TEG was bought from the Beijing Xinyu Kaimeng Electronic Technology Co., Ltd, and the vendor number and dimensions are TEC1-01706T125 and $15 \text{ mm} \times 15 \text{ mm} \times 3.9 \text{ mm}$, respectively.

In the test, the TEG is first sandwiched between a heater and a cooler at the two opposite sides of the device. The heater is a piece of electrical resistor which can convert electricity into heat when there is a current passing and is connected to an adjustable voltage. On the other side, a cooler made of fans is used and settled near the surface to maintain the surface temperature equal to that of the environment. Several thermocouples are mounted at each surface so that the temperature there can be measured synchronously. The voltage output of the TEG is also measured at the same time by the data acquisition system (Agilent 34970, USA). When starting the experiment, the two sides of the TEG are either heated or cooled by the devices connected to it. And an output voltage corresponding to the temperature difference can be obtained. The relationship between them is experimentally measured and shown in figure 9(b). It indicates that the

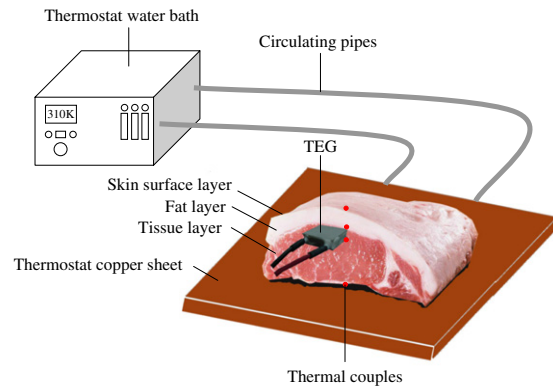


Figure 10. Sketch of *in vitro* experiment of a TEG.

voltage output increases in proportion to the temperature difference between the two junctions. But it is also easy to find out that the capability of energy conversion of such an ordinary TEG is still not high enough. When the temperature difference is 5 K, the voltage output is only about 0.03 V. When the temperature difference reaches 10 K, the voltage output increases to 0.055 V. It is known from our above numerical results that the temperature difference between the body core and the skin surface is generally 5 K. Therefore, one may doubt whether using an implantable TEG to power an IMD will really be feasible. This issue can be addressed by the following experiments and related discussions.

3.2. In vitro experiment of a single TEG

After the test on the energy generation capability of the TEG, we prepared one piece of pork of dimensions $80 \text{ mm} \times 80 \text{ mm} \times 80 \text{ mm}$. The thickness of the skin layer and the fat layer are, respectively, 2 mm and 10 mm. In order to simulate the thermal state of the human body, a copper plate connected with a thermostat water bath at temperature 310 K was placed underneath the muscle tissue of the pork and the surface skin is exposed to the room environment, as shown in figure 10. The same TEG was embedded into this piece of pork parallel with the skin surface. Adiabatic material was used to wrap the four lateral surfaces of the pork. In the experiment, four thermocouples were respectively mounted at the copper surface, cold and hot junction of the TEG and the skin surface of the pork for recording the temperature responses there. Meanwhile, the output voltage of the TEG was also recorded by the same data acquisition system as mentioned above.

The actual environmental temperature is measured as 291 K. When a stable temperature distribution was formed in the pork, the TEG was embedded with its cold side positioned at the interface between the fat and the muscle tissue. At the left-hand side of the line 'start cooling here' in figure 11, is indicated the curve of temperature difference across the TEG and the output voltage of the TEG before intentionally applying external cooling. It is obvious that when the TEG was embedded, a temperature difference across it was immediately established, which could produce a voltage output. Finally, the temperature difference is stabilized at 0.5 K and the output voltage is around 3.3 mV.

At the right-hand side of the line 'start cooling here' in figure 11, is presented the curve of measurement that results

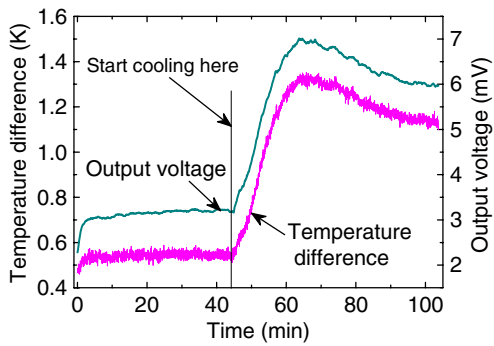


Figure 11. Measurement results across a single TEG in section 3.2. At the left-hand side of the line 'start cooling here', the skin surface is under room environment; at the right-hand side of this line, the skin surface was cooled to 273 K.

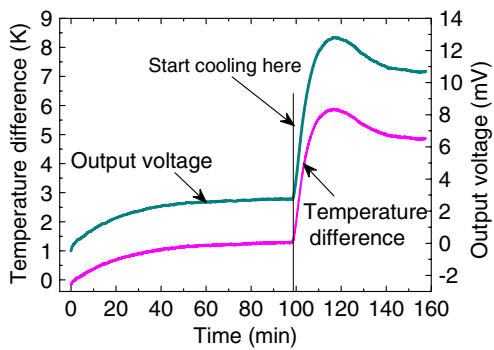


Figure 12. Measurement results across the multi-stage TEG in section 3.3. At the left-hand side of the line 'start cooling here', the skin surface is under room environment; at the right-hand side of the line, the skin surface was cooled to 273 K.

when cooling the skin surface to 273 K. One piece of ice was placed on the skin surface of the pork. Then it can be found that the temperature difference across the TEG and the output voltage increased rapidly reaching its maximum value at a time of about 1200 s. Then both of them gradually decreased and became stable. At this point, the temperature difference is nearly 1.1 K and the TEG output voltage is about 6 mV.

3.3. In vitro experiment using a multi-stage TEG

Based on the analysis as given in section 2.2.6, three other TEGs bought from the same company were connected in series (both electrically and spatially) with the hot junction of one TEG clinging to the cold junction of the next TEG to form a multi-stage TEG. The vendor number and dimensions are TEC1-00706T125 and $10\text{ mm} \times 10\text{ mm} \times 3.9\text{ mm}$, respectively. Due to a different set of modules with a smaller cross section area, the capability of energy generation of a single TEG in this device appears a little weaker than the module tested above. The experiments are repeated by the same procedure as above except at the start. The TEG is embedded before the thermal equilibrium of pork has been reached and the results are shown in figure 12. At the left-hand side of the line indicated by 'start cooling here', the skin surface of the pork is exposed to the room condition at 291 K. In this case, the temperature difference across the TEG as well as its output voltage increased with the time and gradually reached a stable state at 1.3 K and 2.9 mV, respectively.

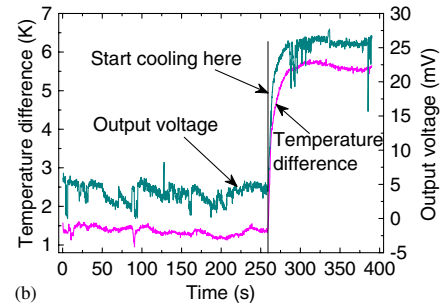
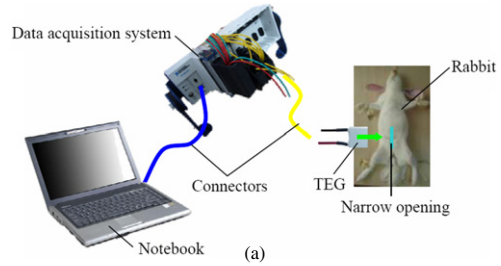


Figure 13. (a) Sketch of the set up of TEG in *in vivo* experiment and (b) temperature difference across the TEG and the output voltage.

At the right-hand side of the line 'start cooling here' is the cooling curve of temperature difference across the TEG and the output voltage of the TEG. In this case, the curve appears to have the same trend as figure 11. Finally, the temperature difference is stabilized at around 5 K and the output voltage is about 11 mV. Clearly, a much evident enhancement on the temperature difference and electricity generation has been realized due to intentionally applied cooling.

Overall, the magnitude for the temperature difference corresponds well with the theoretical prediction. However, because the experiment is performed *in vitro*, there are no blood perfusion and metabolic heat generation in the pork. Therefore, under a similar boundary condition, there exists somewhat a difference between the theoretically predicted temperature differences and the experimental measurements. But such a difference is rather small and highly acceptable in an appropriate range. Interestingly enough, the profile for the instant response curve of temperature difference across the TEG when cooling the skin surface appears as almost the same as figure 7. These results indicate that the theoretical analysis does provide a good overview on the electricity generation capability of an implanted TEG which may help design future medical devices.

3.4. In vivo experiment of one single TEG

To further demonstrate the present concept of using implanted TEGs for generating electricity, *in vivo* experiments were also carried out subsequently. A rabbit weighing 2 kg was selected and the experimental set-up is depicted in figure 13(a). Before the experiment, the rabbit was kept for two weeks in standard laboratory conditions with free water and food. All the procedures performed complied with the International Laboratory Animals Care Convention.

The NI LabVIEW system (NI cDAQ-9172 and NI9205, NI9211) was adopted as the data acquisition. Before implanting the TEG, the rabbit was administered anesthesia

Table 1. The temperature difference and output voltage obtained by simulation and experiments.

Conditions on skin surface		Numerical simulation	Experiment <i>in vitro</i>	Experiment <i>in vivo</i>
Exposed in the environment	ΔT (K)	0.482	0.5	1.3
	V_{output} (mV)	—	3.3	5
Cooled by the ice water	ΔT (K)	1.3	1.2	5.5
	V_{output} (mV)	—	6	25

via an intraperitoneal injection of 20% urethane (5 ml kg^{-1}). After it had fallen into the state of general anesthesia, the rabbit was gently fixed on the operating table. For implantation and measurement purposes, the rabbit hair at its lower abdomen was carefully shaved, where a narrow opening with a length of 0.03 m was made with caution. One piece of TEG, identical to the one in sections 3.1 and 3.2, was implanted into the abdomen from this narrow opening. Meanwhile, two thermocouples were mounted at both the upper and the lower sides of the TEG, respectively. The hot junction of the TEG is attached to the surface of the caecum and its cold junction to the fat layer immediately underneath the skin surface. A suture was subsequently given to close the narrow opening after finishing the implantation. Then both the electrical voltage and the temperature data collection were started at the same time. Four minutes later, the skin surface above the TEG was covered with a packet of ice water contained in a plastic bag. It is found in figure 13 that at the first 260 s, the temperature difference across the TEG is stabilized at about 1.3 K and the output voltage is around 5 mV. After the rabbit skin surface was covered with an ice water bag, the temperature difference across the TEG and the output voltage increase rapidly to its maximum, then gradually level off at 5.5 K and 25 mV. This improving trend of temperature difference is very similar to the result obtained in sections 3.1 and 3.2.

Table 1 enumerates the temperature difference and output voltage obtained in the two different situations by the numerical simulation and experimental measurements *in vitro* and *in vivo*, respectively. One could find that the temperature differences achieved by numerical simulation and experiment *in vitro* are pretty close to each other, which, however, is a little lower than that of the *in vivo* experiment. There are two reasons for this deviation. Firstly, the normal body temperature for a rabbit is 312 K, which is 2 K higher than the corresponding temperature of a human. Meanwhile, the rabbit hairs have been shaved off. Therefore, the temperature gradient from the body core to the skin surface is relatively large. That is why the temperature difference becomes higher when the rabbit skin surface is exposed in the cold environment. Secondly, the fat layer of the rabbit is relatively thin compared with the pork and the setup in the numerical simulation. So, when cooling the skin surface, a larger temperature difference can be expected.

4. Discussion on feasibility of using TEG to drive an IMD

The analysis and measurement as given above revealed that no matter where the implanted TEG is located, there always exists a temperature difference across its two junctions and the temperature difference is related to implantation depth, ambient conditions surrounding the skin surface and the

physiological state of the human body, respectively. In particular, both the theoretical evaluation and the experimental measurement demonstrate that intentionally imposed cooling on the skin surface and adoption of multi-stage TEG play a noteworthy role in obtaining a much higher temperature difference and thus stronger energy generation.

Comparison between cooling and heating the skin surface reveals that the former strategy could gain a much larger temperature difference and thus energy output from an implanted TEG. If the same temperature difference as could be provided by the cooling condition were required, more heat should be applied on the skin surface, which however might cause burns to the tissues. In contrast, cooling the skin surface appears more safe and effective. The multi-stage TEG is another possible option of enhancing electricity generation. Such a configuration could increase the thickness along the direction x and consequently improve the temperature difference across the TEG. All the experiments carried out have proved these two points.

In the numerical calculation, the sizes for the TEG are slightly different from those adopted in the experiments. The main reason for the inconsistency in thickness is that the TEG used in the experiments is sandwiched between two Al_2O_3 ceramic plates which is 0.5 mm thick. The Al_2O_3 ceramic plate has much higher thermal conductivity but less thickness than the bismuth telluride. Therefore, the heat resistance of the Al_2O_3 ceramic plate is quite low, which can be ignored in the numerical simulation. Meanwhile, the theoretical analysis has explicitly instructed that temperature difference across the TEG does not depend on its cross-section area, but only on the thickness of the TEG. Thus, more calculations using different geometrical and thermal parameters based on the simplified TEG model as presented in the numerical simulation do not produce a notable impact on the conclusion.

In addition, the highest environmental temperature used in the numerical simulation was set at 303 K. But in one's daily life, situations with higher temperatures in the environment than the human body also occasionally happen such as in hot sunny weather. Such cases may not be beneficial to the working of a TEG. Therefore, in a high temperature environment, external cooling on the skin surface to guarantee sufficiently high electricity generation for the TEG is strongly recommended.

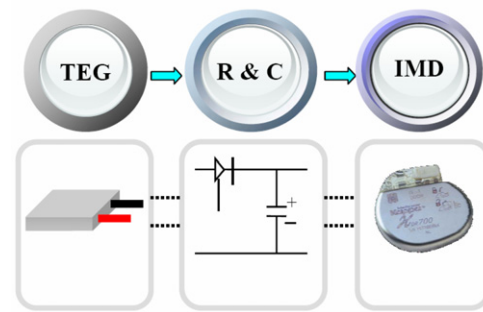
Concerning the practical requirement, we further perform a preliminary evaluation as follows on the ability of using a TEG to power an IMD. The maximal temperature difference as obtained from the foregoing analysis is about 10 K. And from figure 9(b) one can get the information that using an ordinary TEG, only 0.05 V voltage will be gained when the temperature difference reaches 10 K. It has been documented so far that the types of batteries used to power the IMDs

Table 2. Several popular applications and electrical power requirements.

Implanted device	Most common application	Typical power requirement
Cardiac pacemaker	Conduction disorders	30–100 μW
Cardiac defibrillator	Ventricular tachycardia or fibrillation	30–100 μW
Neurological stimulator	Essential tremor	30 μW to several mW
Drug pump	Spasticity	100 μW to 2 mW
Cochlear implants	Help listening	Several μW to 10 mW

generally include: nickel–cadmium batteries, lithium batteries, biofuel cells, nuclear cells and so on where the lowest discharge voltage is a miniaturized enzymatic-biofuel cell with 0.52 V and an operating current of 8.3 μA . Such a magnitude is already sufficient for the operation of implanted sensors and the intermittent transmission of the data collected to an external receiver [18]. Obviously, the results obtained by adopting the present ordinary TEG are unable to guarantee the lowest voltage that an enzymatic-biofuel cell can afford. However, some studies focusing on advancing the efficiency of the TEG have shown that a higher voltage has been achieved under the same temperature difference, such as by using a coin-size coiled-up polymer foil thermoelectric power generator [10]. It was reported that a thermopower of 65 $\mu\text{V K}^{-1}$ could be reached using a single thermocouple. The TEG with a base area of 1 cm^2 at a temperature difference of only 5 K, both of which are typical values for the real use, can generate a voltage of more than 0.8 V. If the screen printing technique is employed, the thermopower of a single thermocouple can realize a value of up to 97 $\mu\text{V K}^{-1}$. Therefore, the voltage output capability could be still further improved. According to these facts, the embedded TEG could possibly achieve the voltage that a traditional battery could provide. This indicates the high feasibility of using TEG to drive an IMD in the near future.

Meanwhile, whether the power produced by the TEG can match the power consumed by the IMDs is another key for this power supply pattern. In fact, the electrical energy required by the IMDs is generally on the level of only several μW to mW, as listed in table 2 [19]. Due to the weak capability of energy conversion and low voltage output of the ordinary TEG as adopted in the experiment, we did not measure its power output. But according to the high performance TEG offered by existing research [10], some analysis on the power output can be carried out as follows. It was found that about 2461 pairs of thermocouple have been successfully disposed in the TEG with a base area of 1 cm^2 . Based on equation (1) under 65 $\mu\text{V K}^{-1}$ thermopower of a single thermocouple, a 5 K temperature difference and a 0.8 V voltage output can be obtained. When the thermopower of a single thermocouple reaches a value of up to 97 $\mu\text{V K}^{-1}$, the voltage output of the TEG would increase to nearly 1.2 V under the 5 K temperature difference. And the impedance of the TEG is quite small, which is about 0.26 Ω for an ordinary TEG as adopted in the experiment. Such values can be ignored compared with the large impedance of IMDs ranging from 0.5 to 100 k Ω [20–23]. It is for this reason that directly measuring the power consumption of an IMD driven by a TEG is still not available at the present stage. However, certain preliminary analysis can still be made. While the voltage is 1.2 V at a 5 K temperature difference, when the

**Figure 14.** The rectifier circuit for the TEG and IMD.

electrical resistance of the IMD takes a minimum of 0.5 k Ω , the current and power output can be calculated as 2.4 mA and 2.88 mW, respectively. When the electrical resistance of the IMD takes a maximum of 100 k Ω , the calculations show that the current and power outputs are, respectively, 12 μA and 14.4 μW . According to these calculations, the embedded TEG could possibly achieve the power that an IMD required. Furthermore, with the tremendous amount of research on many emerging sophisticated nano medical devices, there is an increasing demand for small energy sources. Therefore, what can be offered so far by the present TEG can even be directly used for certain specific situations in the near future.

At the same time, attention should also be paid to various power styles used in an IMD. And the unstable outputs of an implanted TEG may be a problem. In such cases, some capacitors and rectifier circuits can be adopted to store the electrical energy continuously generated by the TEG. A preliminary illustration of such a circuit principle is shown in figure 14. Here, the output of the TEG is led by two insulated conductors to the rectifier circuit which was integrated with an IMD. The rectifier circuit comprises a diode and a super capacitor. Only positive electricity is permitted by the diode. Because of the voltage drop by using the diode, adopting the germanium diode or any other low voltage drop diode which can reduce the waste in voltage is strongly suggested. In regard to the proposal of storing the electricity generated by a TEG, an electric capacitor with a big capacity and numerous charge/discharge times is needed. The super electric capacitor can serve as a good candidate because not only can it satisfy the requirement raised above, but it also allows a low charge voltage suitable for a TEG. In order to fit specific applications, the diode and super electric capacitor should be well chosen and the rectifier circuit should be carefully designed. The electrical connection between the TEG and the IMD can follow the method adopted for the implanted cardiac defibrillator (ICD). It is well known that an ICD is always implanted out of the heart, while its catheter, serving as a conductor of electric

current, goes through into the interior portions of the heart [24]. This connection has been proved to be feasible and reliable and has already been widely used in clinics. What is presented here is only a primary design, employing two gracile wires between the TEG and the IMD and the electric power generated by the TEG can pass through it. At the same time, the insulation and biocompatibility of the wires to the surrounding tissues have to be considered seriously. Therefore it should be pointed out that there is still some time before the present method can be finally used in reality. Tremendous efforts are urgently needed in this area.

Also, the compatibility between a TEG and the human body should be considered seriously. When implanting the TEG into the human body, a membrane, which is provided with good thermoconductivity and biocompatibility with the human body, should be covered on the TEG's surface. Again, some of such efforts can also follow the experiences gathered in previous investigations on classical IMDs.

5. Conclusion

Up to now, significant progress has been made on the material, structure, measurement, simulation and optimization of TEGs. Such devices are becoming more and more attractive power sources which merge the stability, reliability and economy into one assembly to fulfil a wide variety of practical needs. They are playing an ever increasing role in many fields and progressing to the point where they can compete economically with other systems in many aspects [7, 8, 25, 26]. There have been many successful cases for such practices. However, the patterns as justified in this paper have shown certain complementary merits to the traditional battery. First, it can resolve the mismatch between the IMD longevity and the service life of a power supply device to accomplish the permanent object. Secondly, embedding the TEG into the human body could directly absorb the thermal energy from the body core, which will help enhance the utilization ratio of thermal energy. At the same time, the security and stability of this embedded TEG is immune to ambient conditions. Therefore investigation of this embedded TEG for IMDs could become a new area provided by the TEG family.

In this study, theoretical interpretations and numerical simulations were performed to evaluate the temperature difference established across a TEG positioned in the human body and thus its capability for driving an IMD. Parametric analyses were performed to test the effects of various typical physiological factors, the device configuration and the environmental conditions. In particular, externally imposed

cooling was introduced as a flexible way to enhance the energy generation capability as desired. Proof-of-concept experiments were conducted to further demonstrate the feasibility of using the TEG to generate electricity. These results are expected to be a valuable reference for designing an implantable TEG which may actually be used in future clinics.

Acknowledgment

This work is partially supported by the NSFC under Grant 50325622.

References

- [1] Wang F Z, Hua W, Zhang S, Hu D Y and Chen X 2003 *Chin. J. Cardiac Arrhyth.* **7** 2000
- [2] Fan G Z, Yu J and Bai H 2004 *Trends Amplif.* **8** 01
- [3] Holmes C F 2001 *J. Power Source* **97–98** 739
- [4] Davis F and Higson S P J 2006 *Biosens. Bioelectron.* **22** 1224
- [5] Parsonnet V, Berstein A D and Perry G Y 1999 *Am. J. Cardiol.* **66** 837
- [6] Wang W, Jia F L, Huang Q H and Zhang J Z 2005 *Microelectron. Eng.* **77** 223 (in Chinese)
- [7] Chakraborty A, Saha B B, Koyama S and Ng K C 2006 *Int. J. Heat Mass Transfer* **49** 3547
- [8] Xi H X, Luo L A and Fraisse G 2007 *Renew. Sustainable Energy Rev.* **11** 923
- [9] Glatz W, Muntwyler S and Hierold C 2006 *Sensors Actuators A* **132** 337
- [10] Weber J, Potje-Kamloth K, Haase F, Detemple P, Völklein F and Doll T 2006 *Sensors Actuators A* **132** 325
- [11] Rowe D M 1995 *CRC Handbook of Thermoelectrics* (Boca Raton, FL: CRC Press) pp 490 and 494
- [12] Pennes H H 1948 *J. Appl. Phys.* **1** 93
- [13] Deng Z S and Liu J 2002 *ASME J. Biomech. Eng.* **124** 638
- [14] Deng Z S and Liu J 2004 *Comput. Biol. Med.* **34** 495
- [15] http://science.phy.ncu.edu.tw/program_office/fileresult/
- [16] Liu J and Wang C 1997 *Bioheat Transfer* (Beijing: Science Press) p 344 (in Chinese)
- [17] Gui L and Liu J 2004 *6th Int. Symp. on Heat Transfer (Beijing, 15 June 2004)* (Beijing: Higher Education Press)
- [18] Heller A 2004 *Phys. Chem. Chem. Phys.* **6** 209
- [19] Schmidt C L and Skarstad P M 2001 *J. Power Sources* **97–98** 742
- [20] http://www.medtronic.com/crm/performance/references/icd_reference.html
- [21] Zhang Z Y, Li W Y and Wang Z G 2005 *J. IEEE* **27** 45
- [22] Jin J 2003 *Chin. Med. Devices Inform.* **9** 11
- [23] Guedeney D and Bailly A 2001 High impedance leads for implantable medical devices *US Patent* 6181972
- [24] <http://images.healthcenteronline.com/heart/images/article/ACF28.jpg>
- [25] Carlton R D 1966 *IEEE Trans. Vehicular Commun.* **49** 49
- [26] Fleurlat J P, Borshchevsky A, Caillat T and Ewell R 1997 *Energy Convers. Eng. Conf.* **2** 1080